Desheng Shi, Wensai Zhang, Long Liu, Renliang Wang, Zhixiong Huang and Dongyun Guo\*

# Effect of oleic acid on morphologies of BaTi<sub>5</sub>O<sub>11</sub> nanocrystals synthesized by hydrothermal method

https://doi.org/10.1515/ijmr-2022-0490 Received November 30, 2022; accepted March 23, 2023; published online December 14, 2023

**Abstract:** BaTi<sub>5</sub>O<sub>11</sub> nanocrystals were synthesized by a hydrothermal method, and the effect of oleic acid (OA) in the Ba-Ti precursors on morphologies of BaTi<sub>5</sub>O<sub>11</sub> nanocrystals was investigated. As the  $OA/(Ba^{2+} + Ti^{4+})$  molar ratio ranged from 0 to 8, single-phase BaTi<sub>5</sub>O<sub>11</sub> nanocrystals were synthesized at 260 °C for 20 h. When OA reagent was not added to the precursors, rice-like BaTi<sub>5</sub>O<sub>11</sub> nanocrystals were obtained. As the  $OA/(Ba^{2+} + Ti^{4+})$  molar ratio was 1, elongated lath-like BaTi<sub>5</sub>O<sub>11</sub> nanocrystals were synthesized with the width of about 130 nm, thickness of about 50 nm and length of about 400 nm. With increasing the OA/(Ba<sup>2+</sup> + Ti<sup>4+</sup>) molar ratio from 1 to 6, the grain size of elongated lath-like BaTi<sub>5</sub>O<sub>11</sub> nanocrystals gradually decreased. As the OA content increased, the amount of adsorbed OA molecules on the surface of Ti(OH), nucleus increased and hindered the reaction of Ba<sup>2+</sup> ions with Ti(OH)<sub>x</sub> nucleus, which caused the decrease of grain size of lath-like BaTi<sub>5</sub>O<sub>11</sub> nanocrystals. When the BaTi<sub>5</sub>O<sub>11</sub> nanocrystals were synthesized at  $OA/(Ba^{2+} + Ti^{4+})$  molar ratio of 1, they had the largest dielectric constant ( $\varepsilon_{\rm r}$ ) of 40.9 at 5 GHz.

**Keywords:**  $BaTi_5O_{11}$  nanocrystals; Hydrothermal method; Oleic acid; Morphology; Microwave dielectric constant

#### 1 Introduction

As a typical microwave dielectric material, the  $BaTi_5O_{11}$  compound with monoclinic structure has been widely studied for application in microwave communications [1].

\*Corresponding author: Dongyun Guo, School of Materials Science and Engineering, Wuhan University of Technology, Wuhan 430070, P.R. China, E-mail: guody@whut.edu.cn. https://orcid.org/0000-0002-7422-5080

Desheng Shi, Wensai Zhang, Long Liu, Renliang Wang and Zhixiong Huang, School of Materials Science and Engineering, Wuhan University of Technology, Wuhan 430070, P.R. China

Tillmanns firstly reported the existence of BaTi<sub>5</sub>O<sub>11</sub> phase by melting BaO:4TiO2 composition between 1400 and 1500 °C [2]. Negas et al. [3] failed to prepare the BaTi<sub>5</sub>O<sub>11</sub> compound in the subsolidus by melting BaTiO<sub>3</sub>:TiO<sub>2</sub>. O'Bryan and Thomson sintered a mixture of BaO:5TiO2 at 1100 °C, and the major phase of BaTi<sub>5</sub>O<sub>11</sub> was obtained [4]. Ritter et al. [5] firstly synthesized a pure BaTi<sub>5</sub>O<sub>11</sub> phase via an organic precursor route, and predicated that the singlephase BaTi<sub>5</sub>O<sub>11</sub> ceramics should have excellent microwave dielectric properties. Javadpour and Eror also synthesized the single-phase BaTi<sub>5</sub>O<sub>11</sub> compound by a liquid mix technique between 700 and 1100 °C for 4 h [6]. Fukui et al. [7] prepared BaTi<sub>5</sub>O<sub>11</sub> ceramics from an alkoxide-derived powder. The BaTi<sub>5</sub>O<sub>11</sub> ceramics with more than 99 % theoretical density were synthesized by sintering at 1120 °C for 48 h, their dielectric constant ( $\varepsilon_r$ ) and Q volume were 42 and 6100 at 9.7 GHz, respectively, and the temperature coefficients of the resonant frequency ( $\tau_{\rm f}$ ) was 39.3 ppm/°C at 7 GHz. Zhou et al. [8] prepared BaTi<sub>5</sub>O<sub>11</sub> ceramics by a reaction-sintering process at 1100 °C for 6 h with CuO addition, and the BaTi<sub>5</sub>O<sub>11</sub> ceramics had good microwave dielectric properties ( $\epsilon_{\mathrm{r}}$  of 41.2,  $Q \times f$  of 47,430, and  $\tau_{\mathrm{f}}$ of 36 ppm/°C). Jang et al. [9] deposited the  $BaTi_5O_{11}$  thin films on poly-Si/SiO<sub>2</sub>/Si substrates by a magnetron sputtering method, and  $\varepsilon_{\rm r}$  of BaTi $_{\rm 5}$ O $_{\rm 11}$  thin film measured at 100 kHz was about 35. Guo et al. [10] prepared the BaTi<sub>5</sub>O<sub>11</sub> thick films on Pt/Ti/SiO<sub>2</sub>/Si substrates by a laser chemical vapor deposition method, and  $\varepsilon_{\mathrm{r}}$  of  $\mathrm{BaTi_5O_{11}}$  thick film measured at 1 MHz was only 21.4. In our previous research, rice-like BaTi<sub>5</sub>O<sub>11</sub> nanocrystals were synthesized by the hydrothermal method, and  $arepsilon_{
m r}$  of rice-like  ${
m BaTi_5O_{11}}$  nanocrystals was measured to be about 38.9 at 8 GHz [11]. The nanocrystals possess unique physical and chemical properties that are strongly related to their size, shape, and surface chemistry [12]. Oleic acid (OA) has been widely used as a surfactant to tune the shape of BaTiO<sub>3</sub> and SrTiO<sub>3</sub> nanocrystals synthesized by the hydrothermal method [13]. In our previous reports [11, 14, 15], rice-like BaTi<sub>5</sub>O<sub>11</sub> nanocrystals were synthesized by the hydrothermal method without the surfactant in the precursors.

In this study,  ${\rm BaTi_5O_{11}}$  nanocrystals were synthesized by the hydrothermal method, and the effect of OA content

in the precursors on morphologies of  ${\rm BaTi_5O_{11}}$  nanocrystals was investigated. The microwave dielectric properties of  ${\rm BaTi_5O_{11}}$  nanocrystals with different morphologies were analyzed.

# 2 Experimental details

All the reagents were of analytical grade purity and were used without further purification. The detail of synthesizing BaTi<sub>5</sub>O<sub>11</sub> nanocrystals by the hydrothermal method was introduced in our previous articles [14, 15]. In this study, the desired amounts of bis(ammonium lactate) titanium dihydroxide (C<sub>6</sub>H<sub>18</sub>N<sub>2</sub>O<sub>8</sub>Ti, TALH, 50 wt.% in water, Macklin) and Ba(OH)2·8H2O (Sinopharm) were dissolved in deionized water to form the Ba-Ti precursors, and then the OA (Sinopharm) and NaOH (Sinopharm) were added to the Ba-Ti precursors in sequence with continuous stirring. In the initial Ba-Ti precursors, the concentrations of Ba<sup>2+</sup> and Ti<sup>4+</sup> ions were 0.018 and 0.082 mol L<sup>-1</sup>, respectively, the NaOH concentration was  $1 \text{ mol L}^{-1}$ , and the OA/(Ba<sup>2+</sup> + Ti<sup>4+</sup>) molar ratio varied from 0, 1, 2, 4, 6, 8 to 10. The total volume of each Ba-Ti precursor was about 40 mL, and each precursor was put in an autoclave of 60 mL capacity. These precursors were hydrothermally synthesized at 260 °C for 20 h, and then the autoclaves were naturally cooled to room temperature with continuous stirring. After the hydrothermal reactions, the precipitates were centrifuged and washed in sequence with deionized water, cyclohexane and ethanol.

The phase composition of the precipitates was measured by an X-ray diffractometer (XRD, D/MAX-RB, Japan) with scanning speed of 2° min<sup>-1</sup>. Their morphologies were characterized by a field emission scanning electron microscope (FESEM, ZEISS-ULTRA, Germany) and a high-resolution transmission electron microscope (TEM, JEM-2100F, Japan). The infrared spectra of the samples were measured by a Fourier transform infrared spectrophotometer (FT-IR, Thermo Fisher Nicolet 6700, USA). To measure the microwave dielectric properties of BaTi<sub>5</sub>O<sub>11</sub> nanocrystals, a practical medium theory based on the Bruggeman equation was applied to extract the  $\varepsilon_r$  values of BaTi<sub>5</sub>O<sub>11</sub> nanocrystals in composites [16]. The detail of preparing BaTi<sub>5</sub>O<sub>11</sub> nanocrystals/paraffin wax composites was reported in our previous report [11]. The microwave dielectric properties of BaTi<sub>5</sub>O<sub>11</sub> nanocrystals/paraffin wax composites were measured using an Agilent N5230A vector network analyzer (USA) with measuring frequencies ranging from 0.1 to 5 GHz.

#### 3 Results and discussion

Figure 1 shows the XRD results of the precipitates synthesized with different OA content in the Ba–Ti precursors. The XRD patterns were indexed according to the monoclinic BaTi $_5$ O $_{11}$  phase (JCPDS No. 35-0805). When the OA/(Ba $^{2+}$  + Ti $^{4+}$ ) molar ratio ranged from 0 to 8, the single-phase BaTi $_5$ O $_{11}$  precipitates were synthesized within the detection limit of XRD measurement. With increasing the OA/(Ba $^{2+}$  + Ti $^{4+}$ ) molar ratio from 1 to 8, the peak intensity of BaTi $_5$ O $_{11}$  phase slightly decreased. As the precipitate was synthesized at OA/(Ba $^{2+}$  + Ti $^{4+}$ ) molar ratio of 10, only anatase TiO $_2$ 

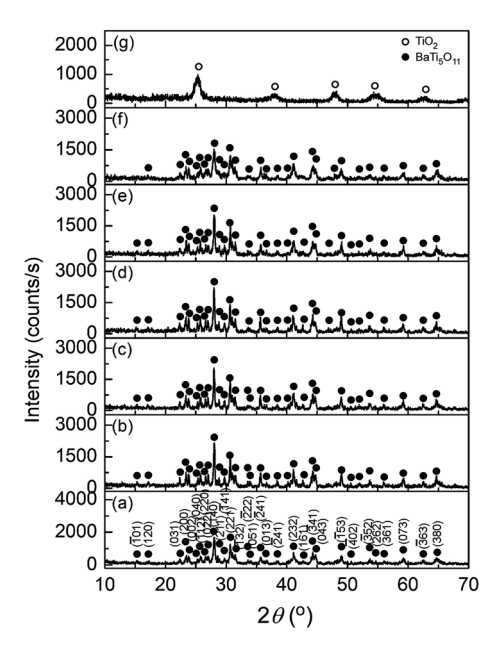


**Figure 1:** XRD patterns of the precipitates synthesized at different molar ratios of  $OA/(Ba^{2+} + Ti^{4+})$ : (a) 0, (b) 1, (c) 2, (d) 4, (e) 6, (f) 8, and (g) 10.

phase was formed. It indicated that the high OA concentration in the precursor could hinder the reaction of  $Ba^{2+}$  and  $Ti^{4+}$  ions to form  $BaTi_5O_{11}$  phase.

Figure 2 displays typical SEM images of BaTi<sub>5</sub>O<sub>11</sub> precipitates synthesized with different OA content in the Ba-Ti precursors. As the BaTi<sub>5</sub>O<sub>11</sub> nanocrystals were synthesized without OA additive, rice-like BaTi<sub>5</sub>O<sub>11</sub> nanocrystals were synthesized, which was the same as in our previous report [11, 13, 14]. When the  $OA/(Ba^{2+} + Ti^{4+})$  molar ratio reached 1, the nanocrystal size obviously increased, and elongated lath-like nanocrystals were formed with a width of about 130 nm, a thickness of about 50 nm and a length of about 400 nm. With increasing the  $OA/(Ba^{2+} + Ti^{4+})$  molar ratio from 1 to 6, the grain size of elongated lath-like nanocrystals decreased, and the number of faceted grains increased. This change was consistent with the XRD results (Figure 1). At high  $OA/(Ba^{2+} + Ti^{4+})$  molar ratio of 8, the irregular BaTi<sub>5</sub>O<sub>11</sub> nanoflakes with thickness of about 20 nm were formed. These results indicated that the OA content in the Ba-Ti precursors seriously influenced the morphologies of BaTi<sub>5</sub>O<sub>11</sub> nanocrystals.

Figure 3 displays typical TEM images of elongated lathlike nanocrystals synthesized at  $OA/(Ba^{2+} + Ti^{4+})$  molar ratios of 1 and 6, and the crystal structure of  $BaTi_5O_{11}$  phase. When the nanocrystals were synthesized at  $OA/(Ba^{2+} + Ti^{4+})$  molar ratio of 1, a typical lath-like nanocrystal was observed, as shown in Figure 3a. The lath-like nanocrystal had width of about 140 nm and length of about 480 nm,

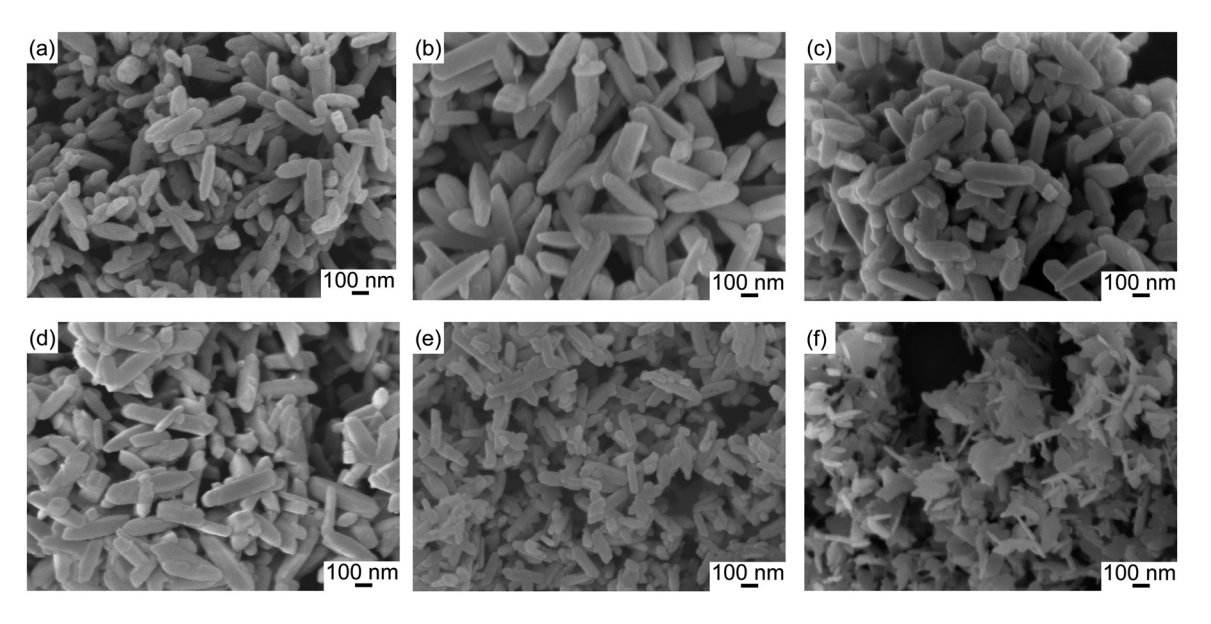


Figure 2: Morphologies of  $BaTi_5O_{11}$  nanocrystals synthesized at different molar ratios of OA/( $Ba^{2+} + Ti^{4+}$ ): (a) 0, (b) 1, (c) 2, (d) 4, (e) 6, and (f) 8.

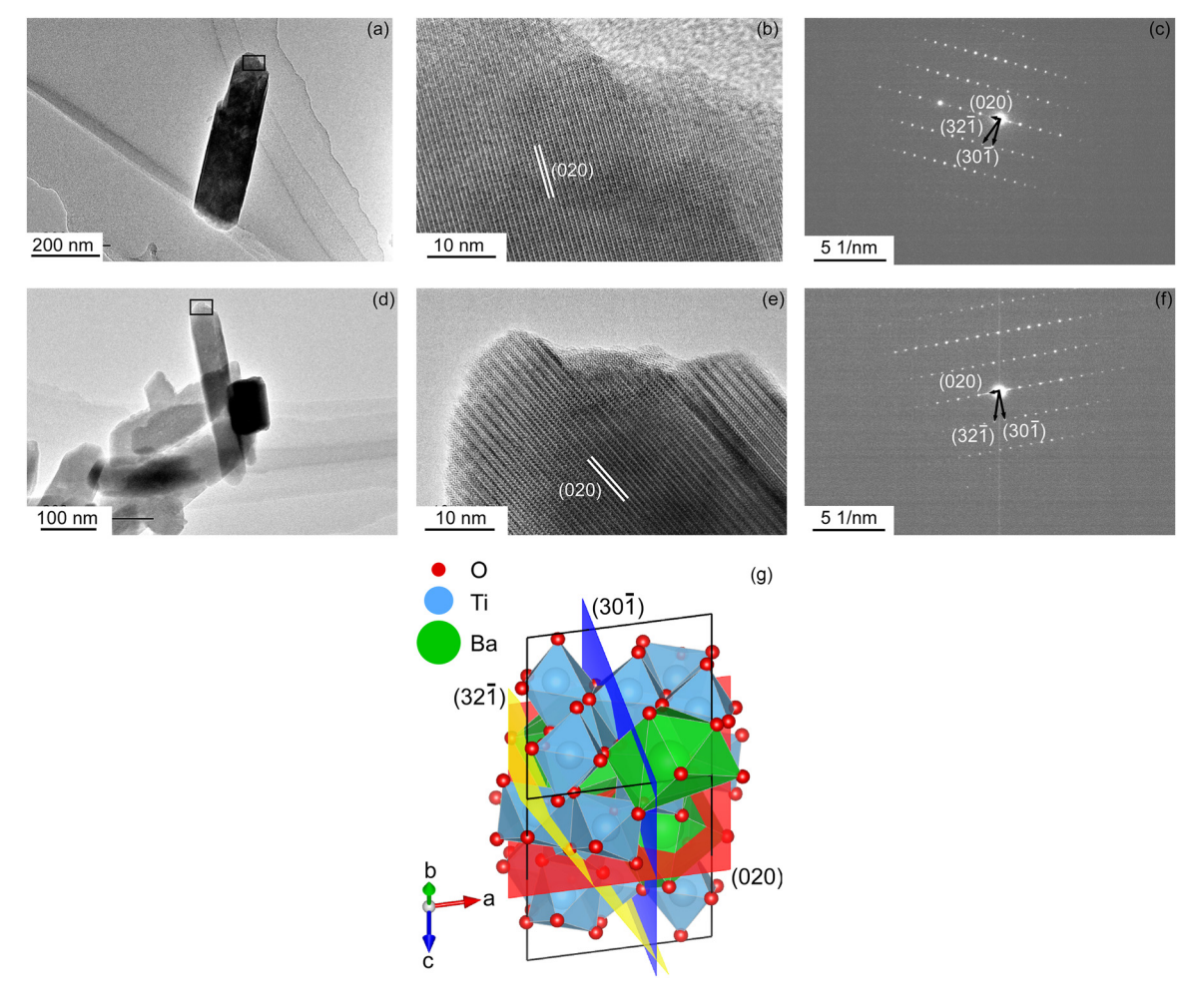
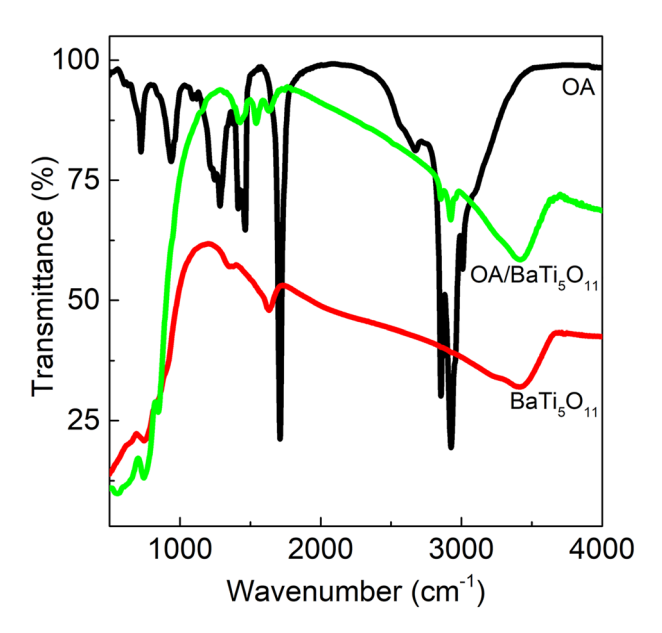


Figure 3: TEM images, high-resolution TEM images and their corresponding selected area electron diffraction (SAED) patterns of BaTi<sub>5</sub>O<sub>11</sub> nanocrystals synthesized at different molar ratios of OA/(Ba $^{2+}$  + Ti $^{4+}$ ): (a, b and c) 1, (d, e and f) 6, and (g) the crystal structure of BaTi $_5$ O $_{11}$  compound.

which was close to the results as shown in Figure 2b. Figure 3b shows a high-resolution TEM image of the circled area in Figure 3a. The interplanar spacing with 0.7087 nm corresponded to the (020) plane (0.7021 nm) of the monoclinic BaTi<sub>5</sub>O<sub>11</sub> phase. Its corresponding selected area electron diffraction (SAED) pattern is shown in Figure 3c. The included angles between the (020) and (301) planes, (020) and (321) planes were measured to be 89.43° and 69.92°, respectively. The included angles between the (020) and  $(30\overline{1})$  planes, (020) and  $(32\overline{1})$  planes were calculated to be 90° and 70.34° based on the monoclinic BaTi<sub>5</sub>O<sub>11</sub> phase (JCPDS No. 35-0805). The theoretical included angles were consistent with the measured angles, which confirmed that single-crystal BaTi<sub>5</sub>O<sub>11</sub> nanocrystal with lath-like morphology was formed. When the nanocrystals were synthesized at  $OA/(Ba^{2+} + Ti^{4+})$  molar ratio of 6, a single lath-like nanocrystal with width of about 50 nm and length of about 300 nm is shown in Figure 3d. It indicated that the nanocrystals became slimmer with increasing the OA content in the precursors. Figure 3e displays a high-resolution TEM image of the circled area in Figure 3e. The interplanar spacing with 0.7051 nm corresponded to the (020) plane of the monoclinic BaTi<sub>5</sub>O<sub>11</sub> phase, and its corresponding SAED pattern is displayed in Figure 3f. According to the Figure 3f, the included angles between the (020) and (301) planes, (020) and (321) planes were measured to be 90.73° and 70.39°, respectively. The measured angles were close to the calculated angles based on the monoclinic BaTi<sub>5</sub>O<sub>11</sub> phase, which indicated that the lath-like nanocrystal belonged to the monoclinic BaTi<sub>5</sub>O<sub>11</sub> phase. Figure 3g shows the crystal structure of monoclinic BaTi<sub>5</sub>O<sub>11</sub> phase with (020), (30 $\bar{1}$ ) and (321) planes. It was drawn with VESTA software [17]. The TEM results confirmed that the BaTi<sub>5</sub>O<sub>11</sub> nanocrystals with lath-like morphology were formed due to the additive of OA reagent.

OA reagent is considered as a typical surfactant to tune the shape of nanocrystals in the hydrothermal process [13]. To identify the effect of OA on the formation of  $\rm BaTi_5O_{11}$  nanocrystals, FT-IR spectra of OA and  $\rm BaTi_5O_{11}$  nanocrystals synthesized at  $\rm OA/(Ba^{2+} + Ti^{4+})$  molar ratios of 0 and 6 were measured, as shown in Figure 4. When the  $\rm BaTi_5O_{11}$  nanocrystals were synthesized with the OA additive, the peaks at 2923 and 2853 cm $^{-1}$  corresponded to the C–H stretching mode of methyl and methylene groups within OA molecules, and the absorption bands of 1541 and 1420 cm $^{-1}$  represented the stretching frequency of the carboxylate group [18]. This result evidently indicated that the OA molecule's carboxylate group chemically bonded with the surface of  $\rm BaTi_5O_{11}$  nanocrystals during the hydrothermal process.



**Figure 4:** FT-IR spectra of OA, and  $BaTi_5O_{11}$  nanocrystals synthesized at  $OA/(Ba^{2+} + Ti^{4+})$  molar ratios of 0 and 6.

A schematic illustration of BaTi<sub>5</sub>O<sub>11</sub> nanocrystal formation in the hydrothermal process with the OA additive is shown in Figure 5. As the NaOH solution was added to the Ba-Ti precursors, Ti(OH), nuclei were formed. In the hydrothermal process, Ba<sup>2+</sup> ions reacted with Ti(OH)<sub>x</sub> nuclei to form the rice-like BaTi<sub>5</sub>O<sub>11</sub> nanocrystals due to its monoclinic crystal structure (Figure 3g). When the OA reagent was added into the Ba-Ti precursors, OA molecules were hydrophobic and adsorbed on the surface of Ti(OH)<sub>x</sub> nuclei to offer the protecting role [19], and the elongated lath-like BaTi<sub>5</sub>O<sub>11</sub> nanocrystals with flat surface were formed. With increasing OA content, the amount of adsorbed OA molecules on the surface of Ti(OH), nucleus increased and hindered the reaction of Ba2+ ions with Ti(OH), nucleus, which caused the decrease of the grain size for lath-like  ${\rm BaTi_5O_{11}}$  nanocrystals. When the OA/(Ba^2+  $\,+\,$ Ti<sup>4+</sup>) molar ratio reached 8, irregular BaTi<sub>5</sub>O<sub>11</sub> nanoflakes were formed. At high  $OA/(Ba^{2+} + Ti^{4+})$  molar ratio of 10, the Ti(OH)<sub>x</sub> nuclei were completely coated with OA molecules,

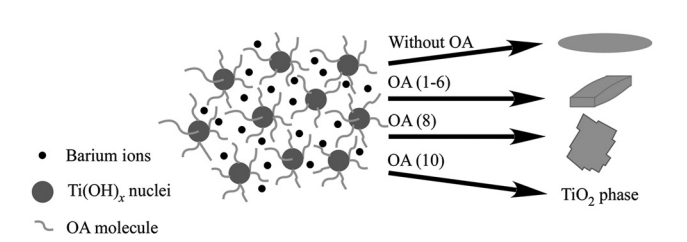


**Figure 5:** Schematic illustration of formation of BaTi $_5$ O $_{11}$  nanocrystals in the hydrothermal process with OA additive.

Ba<sup>2+</sup> ions could not react with Ti(OH), nuclei, and only TiO<sub>2</sub> phase was formed.

The  $\varepsilon_{\rm r}$  values of BaTi<sub>5</sub>O<sub>11</sub> nanocrystals were calculated based on the Bruggeman effective medium theory using the measured dielectric constant of the BaTi<sub>5</sub>O<sub>11</sub> nanocrystals/paraffin wax composites [16]. The Bruggeman equation for effective  $\varepsilon_{\rm r}$  values can be expressed by

$$(1 - f)\frac{\varepsilon_{\rm m} - \varepsilon_{\rm eff}}{\varepsilon_{\rm m} + 2\varepsilon_{\rm eff}} + f\frac{\varepsilon_{\rm p} - \varepsilon_{\rm eff}}{\varepsilon_{\rm p} + 2\varepsilon_{\rm eff}} = 0 \tag{1}$$

where  $\varepsilon_{\rm eff}$ ,  $\varepsilon_{\rm m}$ ,  $\varepsilon_{\rm n}$ , and f represent the effective  $\varepsilon_{\rm r}$  values of the composites, the  $\varepsilon_r$  values of matrix (paraffin wax), the  $\varepsilon_{\mathrm{r}}$  values of  $\mathrm{BaTi_5O_{11}}$  nanocrystals, and the volume fraction of  $BaTi_5O_{11}$  nanocrystals, respectively. When the f value is between 20 and 50 vol.%, the measured  $arepsilon_{
m eff}$  is creditable [16]. The  $\varepsilon_{\rm r}$  values of BaTi<sub>5</sub>O<sub>11</sub> nanocrystals were calculated, and the results are shown in Figure 6. With increasing the measuring frequency from 0.1 to 0.5 GHz, the  $\varepsilon_{\rm r}$  values of BaTi<sub>5</sub>O<sub>11</sub> nanocrystals obviously decreased. When the measuring frequency ranged from 0.5 to 5 GHz, the  $\varepsilon_{\rm r}$  values of BaTi<sub>5</sub>O<sub>11</sub> nanocrystals slightly changed. The  $\varepsilon_{\rm r}$  values of BaTi<sub>5</sub>O<sub>11</sub> nanocrystals at a measuring frequency of 5 GHz are listed in Table 1. As the BaTi<sub>5</sub>O<sub>11</sub> nanocrystals were synthesized at  $OA/(Ba^{2+} + Ti^{4+})$  molar ratio of 1, they had the largest  $\varepsilon_{\rm r}$  value of 40.9 at 5 GHz. With increasing the OA content, the  $\varepsilon_{\rm r}$  values decreased. In our previous report, the  $\varepsilon_r$  value of rice-like BaTi<sub>5</sub>O<sub>11</sub> nanocrystals was about 38.9 (8 GHz), when they were synthesized by hydrothermal

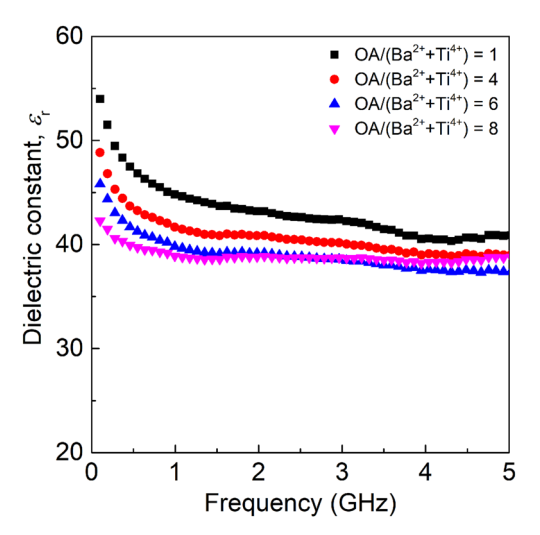


**Figure 6:** Microwave dielectric constant ( $\varepsilon_{\rm r}$ ) of BaTi<sub>E</sub>O<sub>11</sub> nanocrystals synthesized at different molar ratios of OA/(Ba<sup>2+</sup> + Ti<sup>4+</sup>) in the precursors.

Table 1: Dielectric properties of BaTi<sub>5</sub>O<sub>11</sub> nanocrystals at 5 GHz based on the Bruggeman equation.

OA/(Ba <sup>2+</sup> + Ti <sup>4+</sup> ) molar ratios in the precursors	Volume fraction of $BaTi_{5}O_{11}$ nanocrystals ( $f$ , vol.%)	Dielectric constant of ${ m BaTi_5O_{11}}$ nanocrystals $(arepsilon_{ m p})$
1:1	23.89	40.9
1:4	24.05	39.0
1:6	23.80	37.4
1:8	24.05	38.8

method without the additive of OA in the precursors [11]. The  $\varepsilon_r$  value of BaTi<sub>5</sub>O<sub>11</sub> ceramic is about 41, which indicates that the  $\varepsilon_r$  value of lath-like BaTi<sub>5</sub>O<sub>11</sub> nanocrystals is almost the same as that of the bulk  $BaTi_5O_{11}$  ceramics [20].

## 4 Conclusions

BaTi<sub>5</sub>O<sub>11</sub> nanocrystals were synthesized by the hydrothermal method, and their morphology was tuned by the addition of OA reagent in the Ba-Ti precursors. As the OA/(Ba<sup>2+</sup> + Ti<sup>4+</sup>) molar ratio ranged from 0 to 8, the single-phase BaTi<sub>5</sub>O<sub>11</sub> nanocrystals were synthesized. When the OA/(Ba<sup>2+</sup> + Ti<sup>4+</sup>) molar ratio was 1, elongated lath-like BaTi<sub>5</sub>O<sub>11</sub> nanocrystals with the width of about 130 nm, the thickness of about 50 nm and the length of about 400 nm were synthesized. With increasing the OA/(Ba<sup>2+</sup> + Ti<sup>4+</sup>) molar ratio from 1 to 6, the grain size of elongated lath-like BaTi<sub>5</sub>O<sub>11</sub> nanocrystals decreased, and the morphological uniformity of BaTi<sub>5</sub>O<sub>11</sub> nanocrystals worsened. Irregular BaTi<sub>5</sub>O<sub>11</sub> nanoflakes with thickness of about 20 nm were formed at high  $OA/(Ba^{2+} + Ti^{4+})$  molar ratio of 8. As the  $BaTi_5O_{11}$  nanocrystals were synthesized at  $OA/(Ba^{2+} + Ti^{4+})$ molar ratio of 1, they had the largest  $\varepsilon_r$  value of 40.9 at 5 GHz, which was almost the same as that of bulk BaTi<sub>5</sub>O<sub>11</sub> ceramics.

**Research ethics:** Not applicable.

Author contributions: The authors have accepted responsibility for the entire content of this manuscript and approved its submission.

**Competing interests:** The authors state no conflict of interest.

**Research funding:** This work was supported by the National Natural Science Foundation of China (Grant No. 51272195).

Data availability: The raw data can be obtained on request from the corresponding author.

## References

- 1. Higuchi Y., Tamura H. Recent progress on the dielectric properties of dielectric resonator materials with their applications from microwave to optical frequencies. J. Eur. Ceram. Soc. 2003, 23, 2683-2688. https://doi.org/10.1016/S0955-2219(03)00193-6.
- 2. Tillmanns E. Crystal structure of barium titanium oxide (BaTi<sub>5</sub>O<sub>11</sub>). Acta Crystallogr. B 1969, 25, 1444-1452. https://doi.org/10.1107/ S0567740869004195.
- 3. Negas T., Roth R. S., Parker H. S., Minor D. Subsolidus phase relations in the BaTiO<sub>3</sub>-TiO<sub>2</sub> system. J. Solid State Chem. 1974, 9, 297-307. https://doi.org/10.1016/0022-4596(74)90087-5.
- 4. O'Bryan H. M., Thomson J., Plourde J. K. A new BaO-TiO<sub>2</sub> compound with temperature-stable high permittivity and low microwave loss. J. Am. Ceram. Soc. 1974, 57, 450 – 453. https://doi .org/10.1002/chin.197507032.
- 5. Ritter J. J., Roth R. S., Blendell J. E. Alkoxide precursor synthesis and characterization of phases in the barium-titanium oxide system. J. Am. Ceram. Soc. 1986, 69, 155-162. https://doi.org/10.1111/j.1151-2916.1986.tb04721.x.
- 6. Javadpour J., Eror N. G. Raman spectroscopy of higher titanate phases in the BaTiO<sub>3</sub>-TiO<sub>2</sub> system. J. Am. Ceram. Soc. 1988, 71, 206-213. https://doi.org/10.1111/j.1151-2916.1988.tb05849.x.
- 7. Fukui T., Sakurai C., Okuyama M. Effects of heating rate on sintering of alkoxide-derived BaTi<sub>5</sub>O<sub>11</sub> powder. J. Mater. Res. 1992, 7, 192-196. https://doi.org/10.1557/JMR.1992.0192.
- 8. Zhou H., Wang H., Chen Y., Li K., Yao X. Microwave dielectric properties of BaTi<sub>5</sub>O<sub>11</sub> ceramics prepared by reaction-sintering process with the addition of CuO. J. Am. Ceram. Soc. 2008, 91, 3444 - 3447. https://doi.org/10.1111/j.1551-2916.2008.02623.x.
- 9. Jang B., Jeong Y., Lee S., Nahm S., Sun H., Lee W., Yoo M., Kang N., Lee H. Microwave dielectric properties of the BaTi<sub>5</sub>O<sub>11</sub> thin films grown on the poly-Si substrate using rf magnetron sputtering. J. Eur. Ceram. Soc. 2006, 26, 2151-2154. https://doi.org/10.1016/j .jeurceramsoc.2005.09.088.
- 10. Guo D., Ito A., Goto T., Tu R., Wang C., Shen Q., Zhang L. Effect of laser power on microstructure and dielectric properties of BaTi<sub>5</sub>O<sub>11</sub> films prepared by laser chemical vapor deposition method. J. Mater. Sci.: Mater. Electron. 2012, 23, 1961-1964. https:// doi.org/10.1007/s10854-012-0688-7.

- 11. Liu L., Li X., Zou K., Huang Z., Wang C., Zhang L., Guo D., Ju Y. Morphology evolution of BaTi<sub>5</sub>O<sub>11</sub> nanocrystals prepared by hydrothermal method and their permittivity. J. Mater. Sci.: Mater. Electron. 2020, 31, 6883-6889. https://doi.org/10.1007/s10854-020-03250-9.
- 12. Yasui K., Kato K. Influence of adsorbate-induced charge screening, depolarization factor, mobile carrier concentration, and defect-induced microstrain on the size effect of a BaTiO3 nanoparticles. I. Phys. Chem. C 2013, 117, 19632 – 19644. https://doi .org/10.1021/jp312609j.
- 13. Hu L., Wang C., Kennedy R. M., Marks L. D., Poeppelmeier K. R. The role of oleic acid: from synthesis to assembly of perovskite nanocuboid two-dimensional arrays. Inorg. Chem. 2015, 54, 740 - 745. https://doi.org/10.1021/ic5011715.
- 14. Li S., Li X., Zou K., Huang Z., Zhang L., Zhou X., Guo D., Ju Y. Preparation of single-crystalline BaTi<sub>5</sub>O<sub>11</sub> nanocrystals by hydrothermal method. Mater. Lett. 2019, 245, 215-217. https://doi .org/10.1016/j.matlet.2019.02.122.
- 15. Zou K., Liu L., Li X., Li S., Huang Z., Zhang L., Guo D., Ju Y. Effect of NaOH concentration on formation of Ba<sub>4</sub>Ti<sub>13</sub>O<sub>30</sub> and BaTi<sub>5</sub>O<sub>11</sub> nanocrystals prepared by hydrothermal method. Mater. Lett. 2019, 255, 126584. https://doi.org/10.1016/j.matlet.2019.126584.
- 16. Olmedo L., Chateau G., Deleuze C., Forveille J. L. Microwave characterization and modelization of magnetic granular materials. J. Appl. Phys. 1993, 73, 6992-6994. https://doi.org/10.1063/1
- 17. Momma K., Izumi F. VESTA 3 for three-dimensional visualization of crystal, volumetric and morphology data. J. Appl. Crystallogr. 2011, 44, 1272-1276. https://doi.org/10.1107/S0021889811038970.
- 18. Zhou J., Yang Z. Solvothermal growth of sub-10 nm monodispersed BaTiO<sub>3</sub> nanocubes. CrystEngComm 2013, 15, 8912 – 8914. https://doi .org/10.1039/C3CE41549J.
- 19. Ma Q., Mimura K., Kato K. Tuning shape of barium titanate nanocubes by combination of oleic acid/tert-butylamine through hydrothermal process. J. Alloys Compd. 2016, 655, 71-78. https:// doi.org/10.1016/j.jallcom.2015.09.156.
- 20. Zhu S., Dai Y., Pei X. The role of CuO addition in the phase evolution and properties of BaTi<sub>5</sub>O<sub>11</sub> microwave dielectric ceramics prepared by the solid-state reaction method. J. Mater. Sci.: Mater. Electron. 2022, 33, 16406 – 16413. https://doi.org/10 .1007/s10854-022-08532-y.